Arab J. Math. Sc.
Volume 11, Number 1, June 2005
pp.31-54

ON UNIFORM ACCELERATED FLUID FLOW PAST A ROTATING CIRCULAR CYLINDER

M. ANWAR KAMAL AND ABU ZAR A. SIDDIQUI

ABSTRACT. The non-steady flow, due to the uniformly accelerated and rotating circular cylinder from rest in a stationary viscous incompressible fluid is considered. This numerical experiment is made for various values of the Reynolds number in the range from 1 to 350 and several values of rotation parameter α in the range from 0 to 4.5. In this numerical attempt, we have adopted a scheme which consists of two steps. In the first step, the special finite-difference method Dennis [10] is used to approximate the constitutive equations. This method transforms the governing partial differential equations to a system of finite-difference equations which are then solved numerically by S.O.R. iterative method. In the second step, the results obtained are further refined and upgraded by Richardson Extrapolation method. For the purpose of verification, the obtained results are compared on five different grid sizes as well as with those of Collins and Dennis [9] for α=0. The comparison is very favourable.

1. INTRODUCTION

The problem of the fluid flow due to uniformly accelerated and rotating infinite circular cylinder in the stationary incompressible and viscous fluids is of fundamental interest owing to its valuable and large number of applications. For example, in lift enhancement Ackeret [1] and Sayers [24], in the Flettner rotor ship, where the rotating vertical cylinders were employed to develop a thrust normal to any wind blowing past the ship. Secondly, the rotation effects are dominant to control the boundary layer separation discovered by Prandtl [21] and Prandtl and Tietjens [22], Tennant et al [28], and Moore [20]. Thirdly,

the concept of rotating cylinder is very famous and has practical importance in "breakaway" phenomenon Riley [23], Tennant [27], and Walker [29]. Now-a-days, this problem has great dominance in boundary layer control devices such as on the flaps of V/STOL aircraft Cichy [7] and upstream of ship rudders and to overcome separation effects in a subsonic diffuser. Moreover, it has also importance in geophysical motion which is of interest to meteorologists and oceanographers and others who are studying topographic effects in geophysical flow fields.

In present studies, we have discussed the flow behaviour by using two parameters; the rotation parameter α, and R, the Reynolds number. For α=0 (i.e., flow without rotation) the flow becomes accelerated flow past a circular cylinder. This problem has a long history. In 1908, Blasius [2] for the first time considered the general problem for two cases of motion from rest. In case 1, he studied the flow past the impulsively started circular cylinder with uniform velocity, while in case 2, he investigated the flow due to impulsively started circular cylinder with uniform acceleration. For the second case, Goldstein et al [14-15] showed also their efforts numerically. Görlter [16-17], and Watson [30] generalised this theory to other types of variation of the initial velocity of the cylinder. The numerical methods used to solve Navier-Stokes equations for these types of flows were very approximate and valid for all Reynolds number only for leading term in the series solution which is expanded in powers of time. But subsequent terms in the expansion are valid only for infinite Reynolds number.

In 1974, Collins and Dennis [9] studied the second case of Blasius [2] very well and improved and solved them by two techniques. In the first, by the spectral method while in the second, direct integration of Navier-Stokes equations was made which was the extension of the first method. Experimentally this problem was also examined by Tameda [26] in 1972. He measured the time of separation of flow and the growth of the separated wake for Reynolds numbers R^2=97.5, 5850 and 122x10^3.

However, the flow due to uniform translation and rotation with zero acceleration has been investigated numerically as well as experimentally by several researchers for example Badr and Dennis [3-4], Chang and Chern [6], Ece [13] etc. But unfortunately the flow with non-zero acceleration, that is, the flow

due to uniformly accelerated and rotating circular cylinder problem did not receive due attention. It is perhaps due to its sensitivity and complications. It is the one of the reasons for numerical researchers in adopting low order numerical schemes which can provide results and does not converge for large value of t (see for example Collins and Dennis[9]). To overcome this deficiency, we are putting a minute contribution by adopting higher order numerical scheme. Therefore, our scheme is valid for all time, for all Reynolds numbers and there is no problem of divergence. Moreover, our results are in good agreement with those of Collins and Dennis[9] for low values of t when α=0. We shall also try to answer the questions such as: what will be the flow behaviour in the process of vortex shedding in the wake and on the surface of cylinder, the variation of surface forces and pressure development on the surface of cylinder as time passes if we vary rotation speed and its translational speed?

Although the calculations are made for various values of the Reynolds number R in the range $1 \leq R \leq 350$ and several values of α in the range $0 \leq \alpha \leq 4.5$, yet we focus on three values of R namely 1, 10, 349.285 and three values of α namely 2.5, 3, 4.5 and compare the results with Collins and Dennis[9] for small value of t when α=0. The results are presented in graphical form in section 5 in which we have examined the streamlines behaviour, vorticity contours, vorticity variation with time, the variation of surface forces with t for different values of R and α and especially the vortex shedding over the surface cylinder and pressure development in the wake of the cylinder. The formulation and basic analysis of the problem under consideration is given in section 2. The section 3 contains the analysis of transformation of governing equations into a system of finite-difference equations by using special finite difference method and the computational procedure is briefly described in section 4.

2. BASIC ANALYSIS

The continuity and the Navier-Stokes equations for incompressible fluid in dimensional form, in the absence of body force are given as follows:

$$\nabla.\mathbf{V} = 0 \tag{2.1}$$

$$\rho\left[\frac{\partial \mathbf{V}}{\partial t} + (\mathbf{V}.\boldsymbol{\nabla})\mathbf{V}\right] = -\nabla p + \mu\nabla^2\mathbf{V} \tag{2.2}$$

where $\mathbf{V}$ is the fluid velocity vector, ρ the density, p the pressure, and μ the viscosity coefficient.

The mechanics of the problem under consideration can briefly be stated as, the flow is normal to an infinite circular cylinder which is uniformly accelerated and rotating from rest in an infinite stationary viscous incompressible fluid such that the circular cylinder is rotating with angular speed Ω while advancing from right to left with uniform acceleration f. The rotation and translation are started at the same time. Obviously, cylindrical co-ordinate system will be used, where the reference frame is fixed on the cylinder such that origin coincides with the cylinder's centre. However, the coordinate system will be modified further by taking s=lnr. Moreover, the flow is being considered as non-steady, two-dimensional and laminar for all time.

On deforming equation (2.2) into vorticity transport equation, we get

$$-\mu\nabla\times\nabla\times\boldsymbol{\omega}=\boldsymbol{\rho}\left[\frac{\partial\boldsymbol{\omega}}{\partial t}-\nabla\times(\mathbf{V}\times\boldsymbol{\omega})\right] \tag{2.3}$$

where

$$\boldsymbol{\omega}=\nabla x\mathbf{V}. \tag{2.4}$$

In order to normalize the field variables, the following dimensionless parameters can be introduced,

$$x_i^*=\frac{x_i}{c},\mathbf{V}^*=\frac{\mathbf{V}}{\sqrt{fc}},\boldsymbol{\omega}^*=\sqrt{\frac{c}{f}}\boldsymbol{\omega},\quad\text{and}\quad t^*=\sqrt{\frac{f}{c}}t. \tag{2.5}$$

where "*" stands for dimensionless parmeters while f and c signify for uniform acceleration and the radius of the cylinder respectively.

On the introduction of equation (2.5) into equations (2.1) and (2.3), we yield

$$\nabla^*.\mathbf{V}^*=0 \tag{2.6}$$

$$-\nabla^*\times\nabla^*\times\boldsymbol{\omega}^*=\frac{\rho c\sqrt{fc}}{\mu}\left[\frac{\partial\boldsymbol{\omega}^*}{\partial\bar{t}^*}-\nabla^*\times(\mathbf{V}^*\times\boldsymbol{\omega}^*)\right] \tag{2.7}$$

On dropping "*", equations (2.6) and (2.7) can be expressed in components form in the cylindrical polar coordinates system if we use

$$u_r=\frac{1}{r}\frac{\partial\psi}{\partial\theta},u_\theta=-\frac{\partial\psi}{\partial r}, \tag{2.8}$$

and $\boldsymbol{\omega} = [0, 0, E]$ to obtain

$$E = -\nabla^2\psi \tag{2.9}$$

$$\nabla^2 E = \frac{R}{2}\left[\frac{\partial E}{\partial t} + \frac{1}{r}\left\{\frac{\partial\psi}{\partial\theta}\frac{\partial E}{\partial r} - \frac{\partial\psi}{\partial r}\frac{\partial E}{\partial\theta}\right\}\right] \tag{2.10}$$

where R=$\frac{2c\sqrt{fc}}{\upsilon}$, beingReynolds number and $\nabla^2 \equiv \frac{\partial^2}{\partial r^2} + \frac{1}{r}\frac{\partial}{\partial r} + \frac{1}{r^2}\frac{\partial^2}{\partial\theta^2}$.

Our next target is to solve equations (2.9), and (2.10) w. r. t. the following boundary conditions,

$$\begin{cases} \psi = 0, \frac{\partial\psi}{\partial r} = -\alpha, E_w = -\frac{6\psi_1 + H^2 E_1}{2(H^2+H^3)} + \frac{3\alpha H}{2H^2+H^3}, \text{ at } r = 1, \\ \\ \frac{1}{r}\frac{\partial\psi}{\partial r} \to t\sin\theta, \frac{\partial\psi}{\partial\theta} \to t\cos\theta, E \to 0, \text{as } r \to \infty, \end{cases} \tag{2.11}$$

where $\alpha = \Omega\sqrt{\frac{c}{f}}$.

Earlier numerical attempts (e.g., Collins and Dennis[9]) are related to the problem under consideration without rotation of circular cylinder and are studied by using boundary layer techniques which has two major deficiencies: one is that it is valid for high Reynolds number flow and secondly solution no longer converges for large values of time t. The later type of difficulty has been encountered by various authors, for example Sears and Telionis[25], Collins and Dennis[8], Cebeci [5], and Dommelen and Shen[11] and Dommelen[12]. To overcome these difficulties, we adopt higher order numerical scheme which is valid for all Reynolds number, rotation parameter, and specially for all time. Detail of this scheme is given in the following section. This numerical scheme reduces the highly non-linear system of partial differential equations to a system of difference equations, which then can be solved by direct and indirect methods. But we have chosen the SOR-iterative method which accelerates the convergence of the iterative scheme. Henceforth, this numerical procedure is efficient for studies of such type of sensitive flow problems and is straightforward, economical in core storage requirements of a computer, and easy to programme.

3. FINITE-DIFFERENCE METHOD

For convenience, let,

$$s = \ln r. \tag{3.1}$$

Then equations (2.9) and (2.10) would deform as

$$E = -e^{-2s}\Theta^2\psi, \tag{3.2}$$

$$\Theta^2 E = \frac{R}{2}\left[e^{2s}\frac{\partial E}{\partial t} + \frac{\partial \psi}{\partial \theta}\frac{\partial E}{\partial s} - \frac{\partial \psi}{\partial s}\frac{\partial E}{\partial \theta}\right], \tag{3.3}$$

where

$$\Theta^2 \equiv \frac{\partial^2}{\partial s^2} + \frac{\partial^2}{\partial \theta^2}. \tag{3.4}$$

Obviously the boundary conditions given in Eq. (2.11) would deform as,

$$\begin{cases} \psi = 0, \frac{\partial \psi}{\partial s} = -\alpha, E_w = -\frac{6\psi_1 + H^2 E_1}{2(H^2+H^3)} + \frac{3\alpha H}{2H^2+H^3}, & \text{at } s = 0, \\ e^{-s}\frac{\partial \psi}{\partial r} \to t\sin\theta, e^{-s}\frac{\partial \psi}{\partial \theta} \to t\cos\theta, E \to 0, & \text{as } s \to \infty, \end{cases} \tag{3.5}$$

where $s = 0$ represents the surface of the cylinder. E_w is for vorticity on the surface of the cylinder while the subscript 1 denotes the point one cell away to the cylinder's surface.

We shall use the following notation. The grid size along s-, θ-, and t-directions, are taken by H, K_1, K_2 respectively, and the points (s_0, θ_0, t_0), (s_0+H, θ_0, t_0), (s_0, θ_0+K_1, t_0), (s_0-H, θ_0, t_0), (s_0, θ_0-K_1, t_0), (s_0, θ_0, t_0+K_2), (s_0, θ_0, t_0-K_2) are represented by the subscripts 0, 1, 2, 3, 4, 5, 6 respectively. Moreover, the grid which we adopted to discreatize the whole domain of computation is given in figure 1.

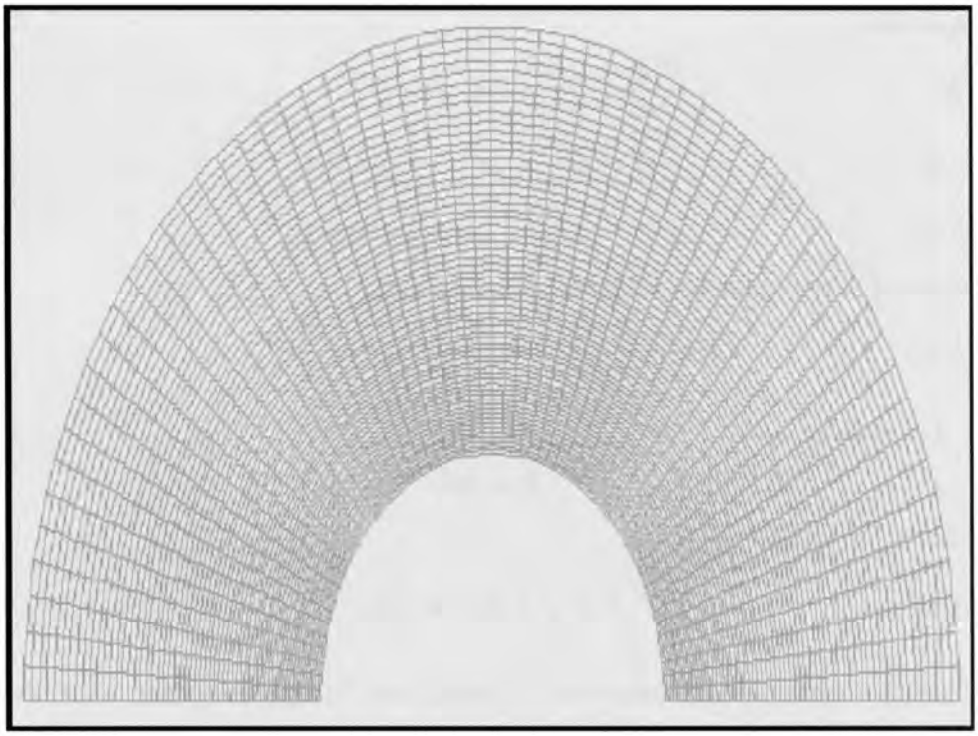

Figure 1. The meshing of computational domain.

In order to approximate equation (3.2), we employ standard central difference formulation at the point "0", that is,

$$\frac{1}{H^2}\psi_1 + \frac{1}{K_1^2}\psi_2 + \frac{1}{H^2}\psi_3 + \frac{1}{K_1^2}\psi_4 - \left(\frac{2}{H^2} + \frac{2}{K_1^2}\right)\psi_0 = -e^{2s_0}E_0 \tag{3.6}$$

The variation in finite-difference formulation, at the point "0", appears in approximating equation (3.3), which can be splitted into the following three equations,

$$\frac{\partial^2 E}{\partial s^2} + B\frac{\partial E}{\partial s} = A(s,\theta,t) \tag{3.7}$$

$$\frac{\partial^2 E}{\partial \theta^2} + C\frac{\partial E}{\partial \theta} = -\frac{1}{2}A(s,\theta,t) \tag{3.8}$$

$$L\frac{\partial E}{\partial t} = -\frac{1}{2}A(s,\theta,t) \tag{3.9}$$

equations,

$$\frac{\partial^2 E}{\partial s^2} + B\frac{\partial E}{\partial s} = A(s,\theta,t) \tag{3.7}$$

$$\frac{\partial^2 E}{\partial \theta^2} + C\frac{\partial E}{\partial \theta} = -\frac{1}{2}A(s,\theta,t) \tag{3.8}$$

$$L\frac{\partial E}{\partial t} = -\frac{1}{2}A(s,\theta,t) \tag{3.9}$$

where A is the unknown arbitrary function and

$$B = -\frac{R}{2}\frac{\partial \psi}{\partial \theta}, C = \frac{R}{2}\frac{\partial \psi}{\partial s}, L = -\frac{R}{2}e^{2s}. \tag{3.10}$$

Let us introdue

$$E = \lambda e^F \tag{3.11}$$

where

$$F = \frac{1}{2}\int_{s_0}^{s} B(x,\theta,t)dx. \tag{3.12}$$

Then the equation (3.7) takes the following form by approximating the derivatives involved by central-differences:

$$(\lambda_1 + \lambda_3 - 2\lambda_0) - \left[\frac{1}{2}\left(\frac{\partial B}{\partial s}\right)_0 + \frac{1}{4}B_0^2\right]\lambda_0 H^2 = A_0 H^2. \tag{3.13}$$

To approximat equation (3.8) along $\theta-$direction, let

$$E = \mu e^G \tag{3.14}$$

where

$$G = \frac{1}{2}\int_{\theta_0}^{\theta} C(s,x,t)dx \tag{3.15}$$

and the equation (3.8) will take the form

$$\frac{H^2}{K_1^2}(\mu_2 + \mu_4 - 2\mu_0) - \left[\frac{1}{2}\left(\frac{\partial C}{\partial \theta}\right)_0 + \frac{1}{4}C_0^2\right]\mu_0 H^2 = \frac{A_0}{2}H^2 \tag{3.16}$$

Next if we approximate equation.(3.9) simply by standard central difference approximation, we get,

$$\frac{L_0 H^2}{2K_2}[E_5 - E_6] = -\frac{A_0}{2}H^2 \tag{3.17}$$

By adding Equations (3.10), (3.11), and (3.12) and using argument that $\lambda_0 = \mu_0 = E_0$, we get

$$\left[\lambda_1 + \lambda_3 - 2E_0 - \frac{1}{4}E_0 B_0^2 H^2\right] + \left[\frac{H^2}{K_1^2}(\mu_2 + \mu_4 - 2E_0) - \frac{1}{4}E_0 C_0^2 H^2\right] + \frac{L_0 H^2}{2K_2}[E_5 - E_6] = 0, \tag{3.18}$$

In order to express λ and μ back in terms of E, it can be done from the definitions. It is found that

$$\lambda_i = E_i e^{F_i}, \mu_j = E_j e^{G_j} \tag{3.19}$$

where

$$\begin{cases} F_i = \frac{1}{2}\int_{s_0}^{s_i} B(x, \theta_0, t_0)dx, \\ \\ G_j = \frac{1}{2}\int_{\theta_0}^{\theta_j} C(s_0, x, t_0)dx \end{cases} \tag{3.20}$$

such that i=1, 3, while j=2, 4

Now we can replace λ_i, and μ_j by expressions involving E_i, and E_j respectively, but they will involve exponential coefficients.

We, next, expand the above exponentials in powers of their arguments keeping the truncation error of order H^4, and $H^2K_1^2$. In expanding the exponents we neglect the terms of order H^4, and $H^2K_1^2$and higher order. After some simplifications under above arguments and using the Taylor theorem, we obtain:

$$\lambda_1 + \lambda_3 = \left[1 + \frac{H^2}{4}\left(\frac{\partial B}{\partial s}\right)_0 + \frac{B_0^2 H^2}{8}\right][E_1 + E_3] + \frac{B_0 H}{2}[E_1 - E_3] \tag{3.21}$$

and

$$\mu_2 + \mu_4 = \left[1 + \frac{K_1^2}{4}\left(\frac{\partial C}{\partial \theta}\right)_0 + \frac{C_0^2 K_1^2}{8}\right][E_2 + E_4] + \frac{C_0 K_1}{2}[E_2 - E_4] \tag{3.22}$$

Introducing equations (3.21) and (3.22) into equation (3.18), we get,

$$\left[1+\frac{B_0H}{2}+\frac{B_0^2H^2}{8}\right]E_1+\left[\frac{H^2}{K_1^2}+\frac{C_0H^2}{2K_1}+\frac{C_0^2H^2}{8}\right]E_2 + \left[1-\frac{B_0H}{2}+\frac{B_0^2H^2}{8}\right]E_3+\left[\frac{H^2}{K_1^2}-\frac{C_0H^2}{2K_1}+\frac{C_0^2H^2}{8}\right]E_4 + \frac{L_0H^2}{2K_2}[E_5-E_6]-\left[2+\frac{2H^2}{K_1^2}+\frac{B_0^2H^2}{4}+\frac{C_0^2H^2}{4}\right]E_0=0 \tag{3.23}$$

4. COMPUTATIONAL PROCEDURE

Equations (3.6) and (3.23) can be written in the following form,

$$R_1\psi_1+R_2\psi_2+R_3\psi_3+R_4\psi_4+R_5E_0-\psi_0 = 0 \tag{4.1}$$

$$T_1E_1+T_2E_2+T_3E_3+T_4E_4+T_5E_5+T_6E_6-E_0 = 0 \tag{4.2}$$

where

$$R_1=R_3=\frac{1}{H^2Z_1}, \qquad R_2=R_4=\frac{1}{K_1^2Z_1},$$
$$R_5=\frac{e^{2s_0}}{Z_1}, \qquad Z_1=\left[\frac{2}{H^2}+\frac{2}{K_1^2}\right],$$
$$T_1=\frac{1+\frac{B_0H}{2}+\frac{B_0^2H^2}{8}}{Z_2}, \qquad T_2=\frac{\frac{H^2}{K_1^2}+\frac{C_0H^2}{2K_1}+\frac{C_0^2H^2}{8}}{Z_2},$$
$$T_3=\frac{1-\frac{B_0H}{2}+\frac{B_0^2H^2}{8}}{Z_2}, \qquad T_4=\frac{\frac{H^2}{K_1^2}-\frac{C_0H^2}{2K_1}+\frac{C_0^2H^2}{8}}{Z_2},$$
$$T_5=\frac{L_0H^2}{2K_2}=-T_6, \qquad Z_2=2+\frac{2H^2}{K_1^2}+\frac{B_0^2H^2}{4}+\frac{C_0^2H^2}{4}.$$

The set of equations (4.1) and (4.2) is solved then iteratively by the point S. O. R iterative procedure Hildebrand [18], subject to the appropriate boundary conditions given in (3.5).

The above procedure is repeated until convergence is obtained according to the criterion,

$$\max\left|E_0^{(m+1)}-E_0^{(m)}\right|<10^{-5}, \max\left|\psi_0^{(m+1)}-\psi_0^{(m)}\right|<10^{-5},$$

where superscript 'm' represents the number of iteration.The results obtained are further refined and enhanced up to the order four by Richardson's extrapolation method, see Jain [19].

5. CALCULATED RESULTS AND DISCUSSION

The calculations were made for various values of Reynolds number R in the range $1 \leq R \leq 350$ and the rotation parameter in the range $0 \leq \alpha \leq 4.5$. The results have been found for the following five grid sizes

(a) $H=1/10$, $K_1=\pi/10$, $K_2=1/130$

(b) $H=1/20$, $K_1=\pi/20$, $K_2=1/130$

(c) $H=1/30$, $K_1=\pi/30$, $K_2=1/130$

(d) $H=1/40$, $K_1=\pi/40$, $K_2=1/130$

(e) $H=1/60$, $K_1=\pi/60$, $K_2=1/130$

But for the purpose of discussion, we focus on four values of R namely 1, 10, 100, and 349.285. The accuracy of the numerical results is checked by comparing the results on different grid sizes for vorticity E and stream function ψ, for various values of R and as mentioned above. In the early stage of flow development, the highly viscous effects and generation of the secondary flows have been observed. That is why, we focus ourselves not only to study in detail the streamlines and eddies behaviour in the time $t<1$ but also we examine their behaviour for time $t>1$. Streamlines are presented graphically in figures 2-10, which show how secondary flow is produced and how it takes the shape with the variation of rotation parameter and time t, specially in the early stages of time. From the studies of these graphs, we observe that secondary flows are produced in the early stages and they vary with R. If we fix and vary R we observe that closed streamlines will remain dominant for longer time. In the early stages of the flow it seems to be very complex and formation of secondary flows is very progressive, for example see figures 5(a), 6(a), 7(a), 8(a), and 9(a). So one can conclude that the secondary flows, which occur in form of closed streamlines and which produce in early stage of fluid motion, remain dominant for longer time as R increases, for fix value of α.

If we fix R and vary α and examine the flow behaviour then illustrations show that the radius of closed streamlines increases for earlier stage while it will continue to decrease as time passes.

The variation of maximum value of streamfunction, ψ_{max} will fluctuate for fixed value of R and t at different values of α. But ψ_{max} also increases at fix value of t and on increasing R as shown in figures 2 to 10. Moreover, it is observed that ψ_{max} varies linearly with t for all values of α.

The behaviour of curves of constant vorticity with the change of R, α, and t is also examined. For the purpose of discussion, we have selected four time levels t=0.046, 0.1, 0.154, and 0.993 for the values of R and α mentioned above. Graphically their behaviour is given in figures 11 to 13. On analysis of the graphs, one can observe that there is no secondary vortex for low Reynolds number for all time before and after the rotation of the circular cylinder as shown in figure 6. When α=0 and R is moderate the situation is different, a pair of secondary vortices produces and these vortices remain isolate before t=0.069 as shown in figure 11(a). But at and after this time this pair by passing through the variety of shapes becomes single vortex at t=0.993 as shown in figure 11(b-d). Moreover, when R increases further the secondary vortices remain isolate till t=0.154. If more increase in R is made i.e., R^2=1.22x10^5 then the time of dissolving of vortices also increases viz., t=1.438. Thus it is found that the secondary vortices in pair are produced in early stage of flows and are dissolved and merged into single big diameter vortex depend upon R and t. When R increases the merge time increases and diameter vortex increases as time passes sometime and then again they occur after certain time. This process varies with the variation with the variation of R. When α increases then one can observe that the vortices are damped and compressed and their radius decreases with the increase of time as shown in figures 12 and 13. The maximum values of vorticity E_M shifts to higher value of time t, that is, E_M occurs at larger time as rotation parameter is increased as shown in figure 13 for α=4.5 respectively.

Figure 14 indicates the variation of minimum vorticity for θ=15° for R=1 and 349.285 and α=2.5 and 4.5. It is observed that the minimum value of vorticity E_{min} fluctuates as time passes. It decreases as either rotation parameter or Reynolds number R increases.

The variation of drag and lift on the surface of the cylinder with respect to time t is also examined for different values of R and α as shown in figures 15 and 16. It can be observed that drag increases as R increases for fix value

of α as shown in figure 15, while situation is vice versa for lift. Here to overcome lift decline, the rotation acts as a vital role. If the rotation parameter increases keeping R as constant we observe that the drag decreases while the lift increases as shown in figures 15 and 16.

The loading effects on the surface of the cylinder is one of our main points of studies, so we have also examined the variation of pressure on the cylinder's surface for various values of the flow parameters and the results are displayed in figures 17. The figure 17(a) illustrates the variation of the pressure on the surface of the cylinder when the cylinder is not rotating while figures17(b-d) represent pressure's variation when rotation is imposed and varies. We also examine that the pressure in the wake and it is observed that it decreases as time passes. This situation does not depend upon whether cylinder is rotating or not. Moreover, the pressure in the wake also decreases strictly and non-linearly as the rotation increases. However, the pressure at front stagnation point remains nearly unaltered as the flow parameters R and α vary and as well as time passes. Figures 17(b-d) show that if the rotation of cylinder begins to fluctuate while it does not occur when rotation tends to stop. Moreover, when α=0 the variation of the pressure on the surface of a cylinder agrees well with that of Collins and Dennis [8].

Finally, the variation of vorticity over the surface of the cylinder with respect to θ is investigated for various values of time t and different values of Reynolds number R and rotation parameter α as shown in figures 18 and 19. In Collins and Dennis[9] at page 479 , it is stated, "The integration terminated soon after (at t=3.2) because of its failure of converge." But our numerical scheme converges for all values of Reynolds number R as well as for t$\geq$0 including t=3.2, when α =0. Figures 18 and 19 show that our results are in good agreement with those of Collins and Dennis[9]. For large values of t, the results are also displayed graphically for α=0 as well as for α=4.5 in figures 19 and 20(b).

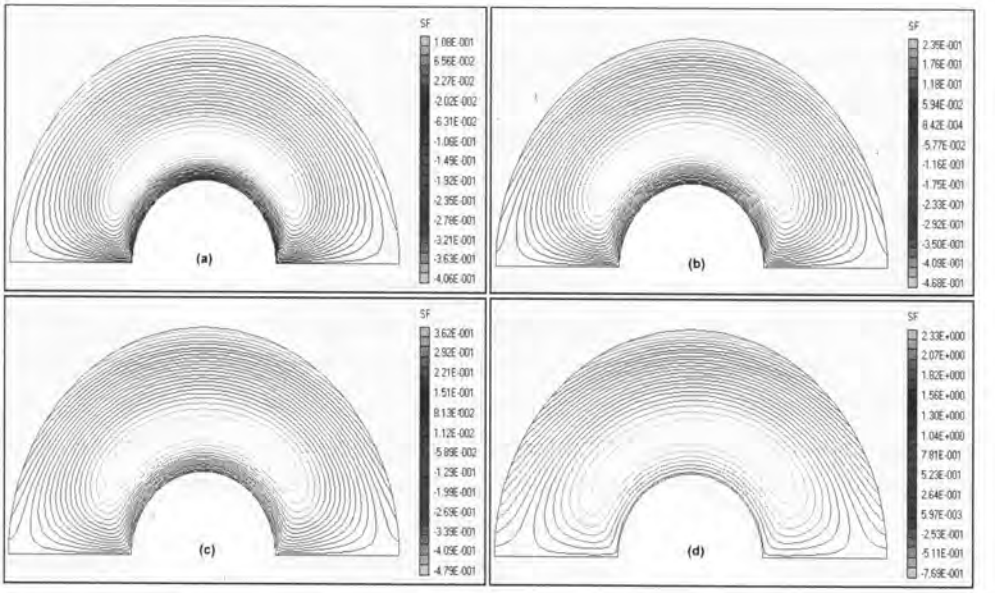

Figure 2. Streamlines for R=1, α=2.5 at time levels (a) t=0.046 (b) t=0.1 (c) t=0.154 (d) t=0.993.

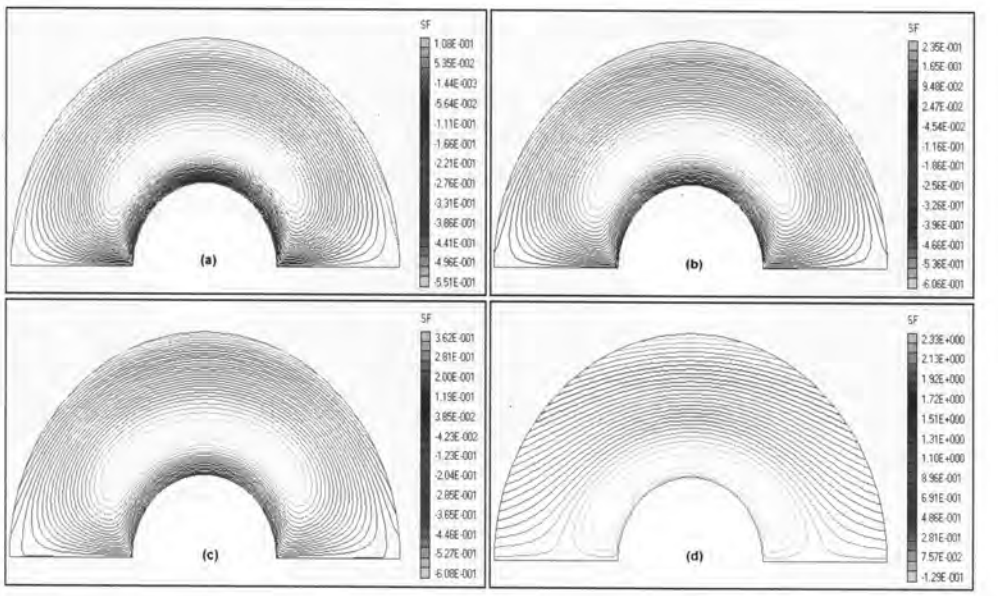

Figure 3. Streamlines for R=1, α=3.0 at time levels (a) t=0.046 (b) t=0.1 (c) t=0.154 (d) t=0.993.

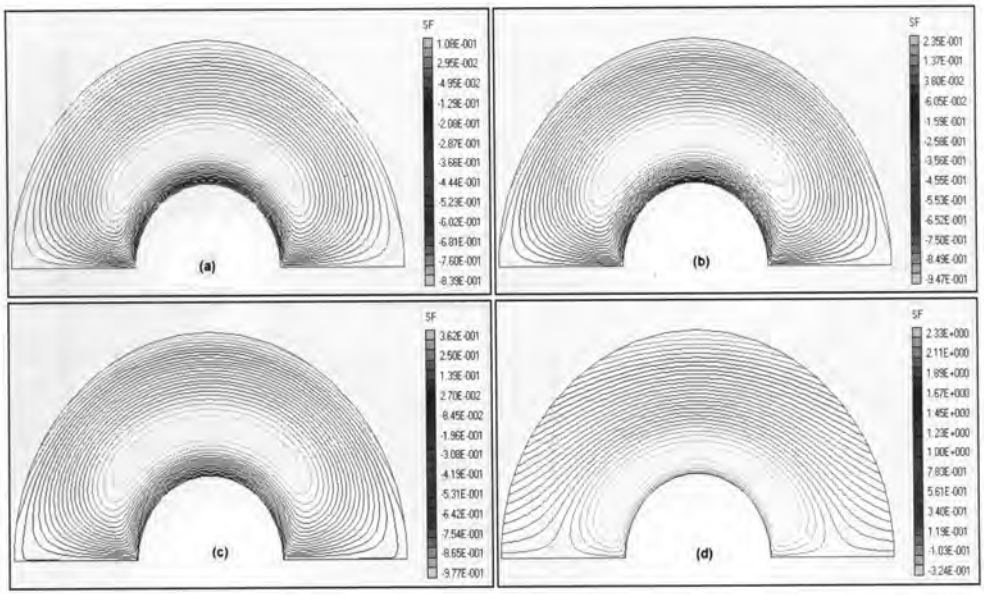

Figure 4. Streamlines for R=1, α=4.5 at time levels (a) t=0.046 (b) t=0.1 (c) t=0.154 (d) t=0.993.

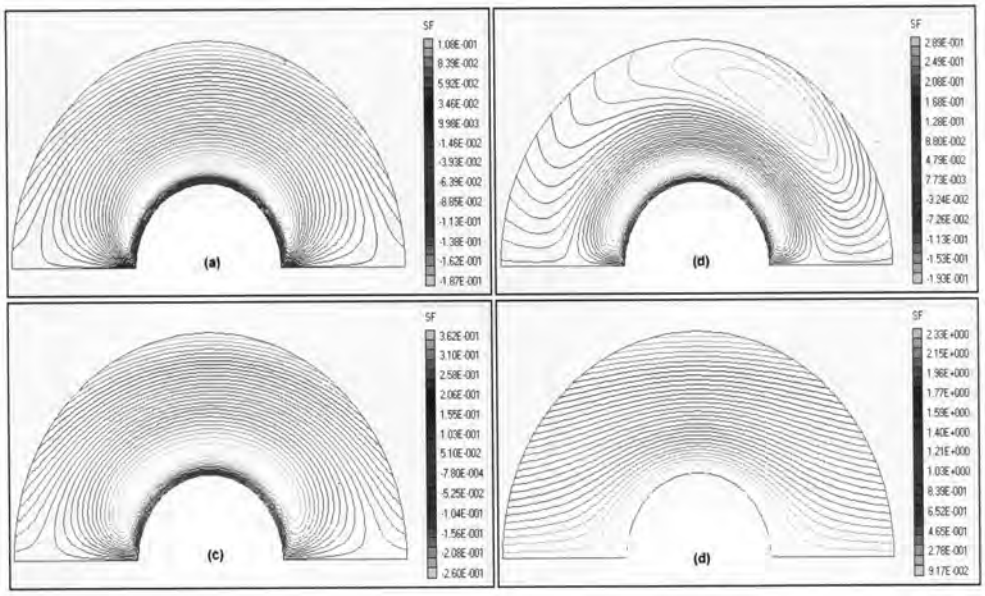

Figure 5. Streamlines for R=10, α=2.5 at time levels (a) t=0.046 (b) t=0.1 (c) t=0.154 (d) t=0.993.

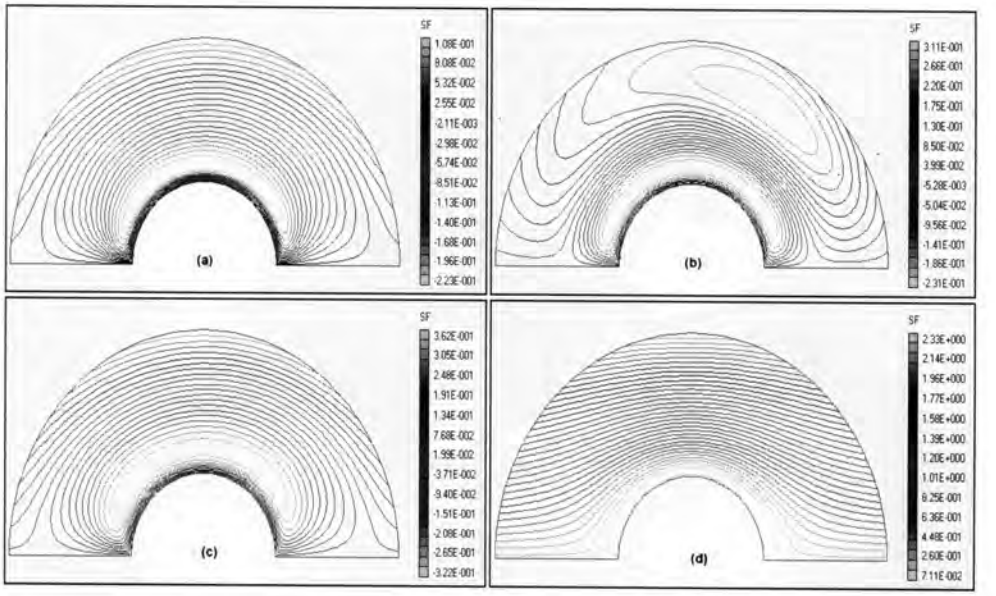

Figure 6. Streamlines for R=10, α=3.0 at time levels (a) t=0.046 (b) t=0.1 (c) t=0.154 (d) t=0.993.

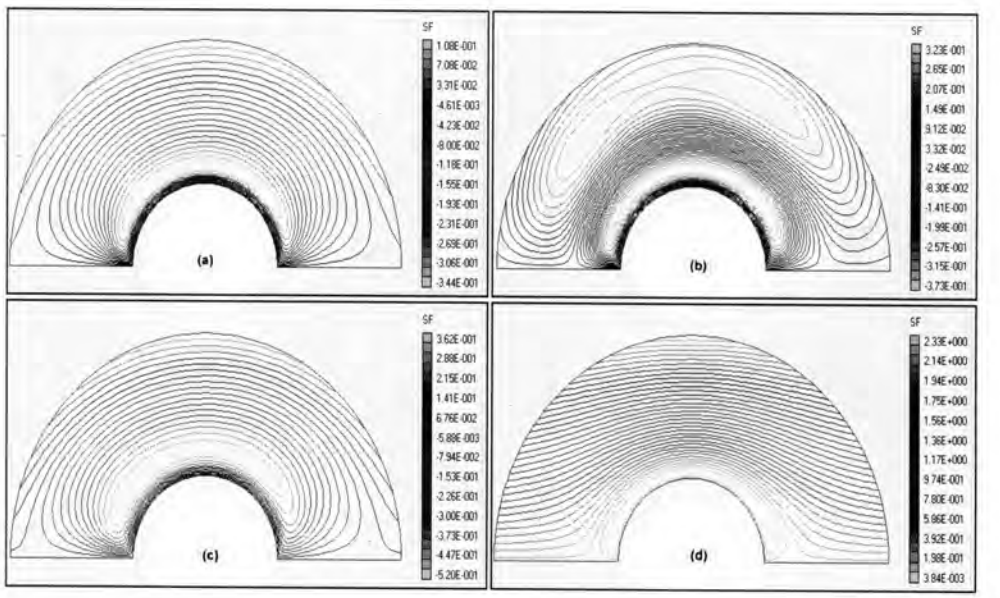

Figure 7. Streamlines for R=10, α=4.5 at time levels (a) t=0.046 (b) t=0.1 (c) t=0.154 (d) t=0.993.

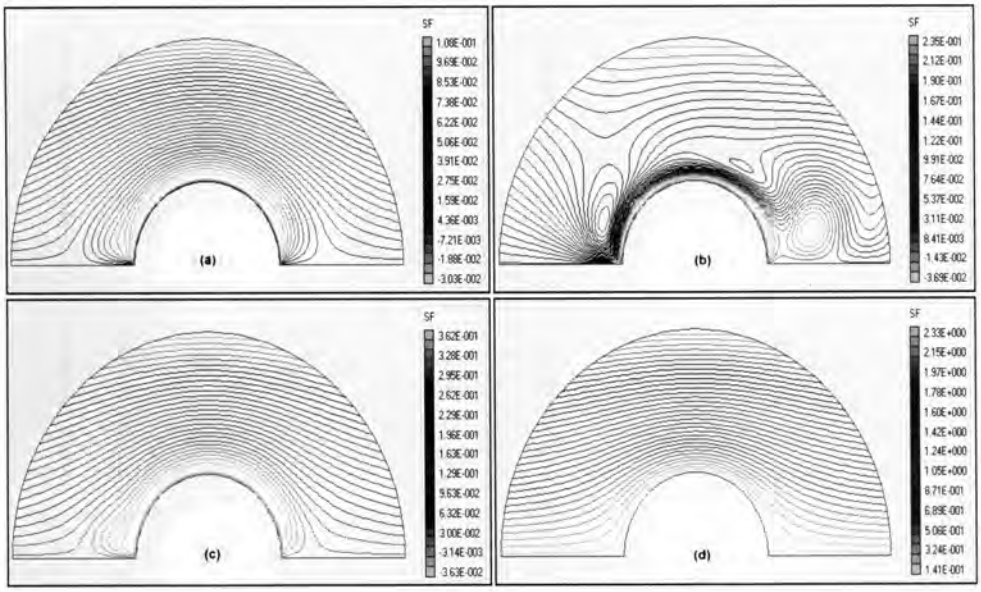

Figure 8. Streamlines for R=349.285, α=2.5 at time levels (a)t=0.046 (b)t=0.1 (c)t=0.154 (d)t=0.993.

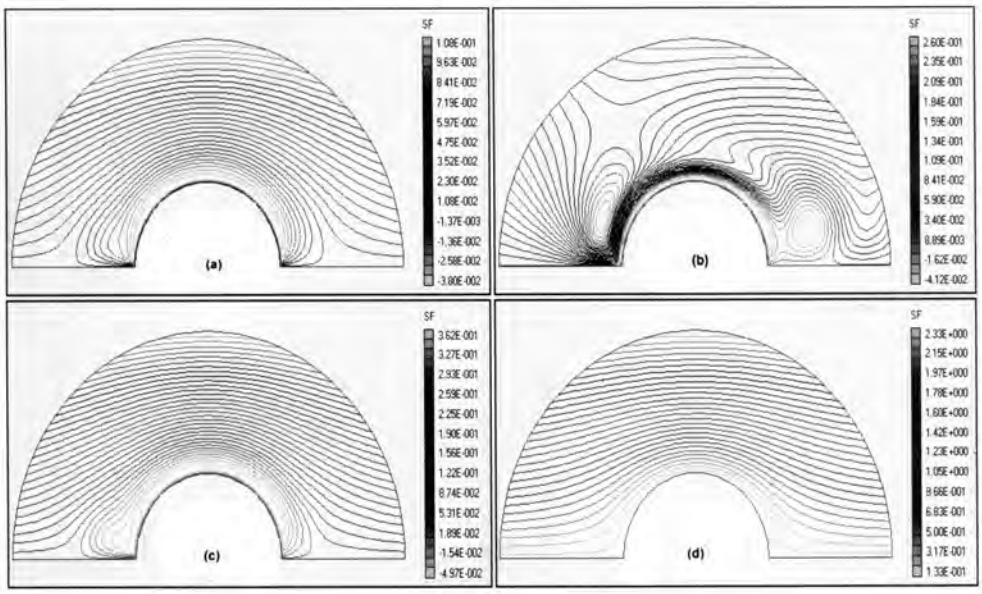

Figure 9. Streamlines for R=349.285, α=3 at time levels (a)t=0.046 (b)t=0.1 (c)t=0.154 (d)t=0.993.

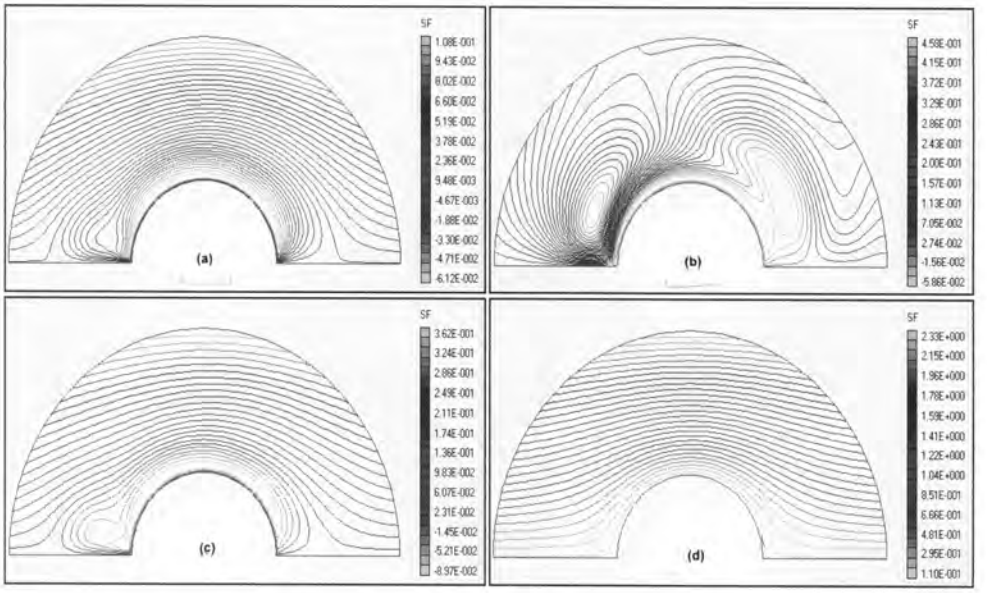

Figure 10. Streamlines for R=349.285, =4.5 at time levels (a)t=0.046 (b)t=0.1 (c)t=0.154 (d)t=0.993.

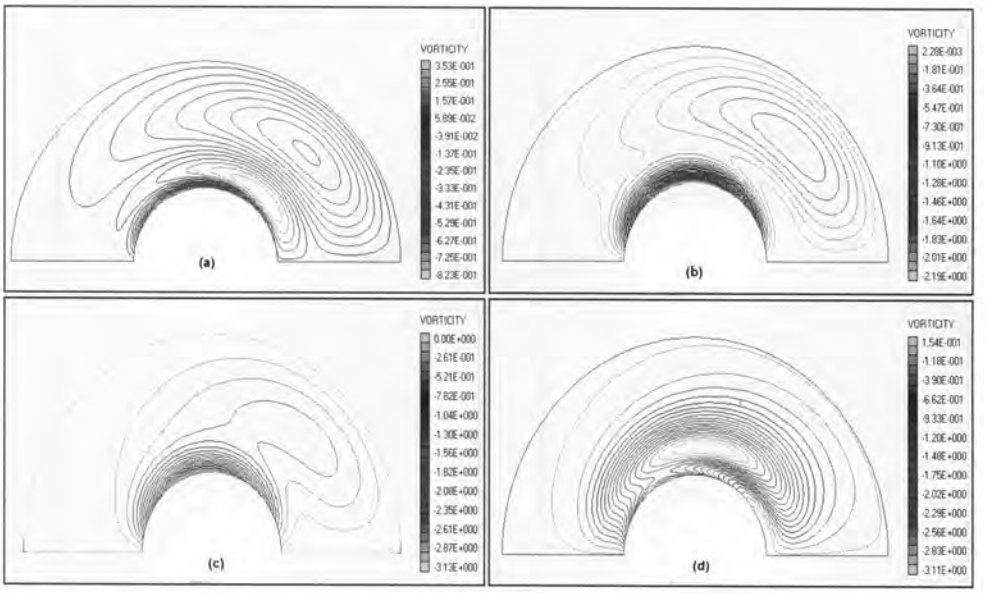

Figure 11. The lines of constant vorticity for R=10, α=0 at time levels (a) t=0.046 (b) t=0.1 (c) t=0.154 (d) t=0.993.

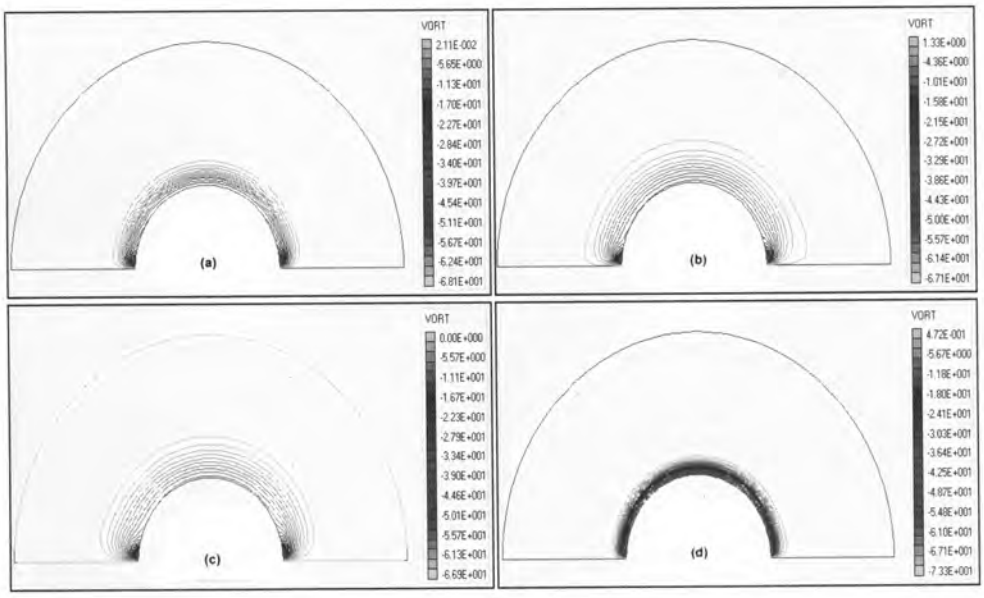

Figure 12. The lines of constant vorticity for R=10, α=2.5 at time levels (a) t=0.046 (b) t=0.1 (c) t=0.154 (d) t=0.993.

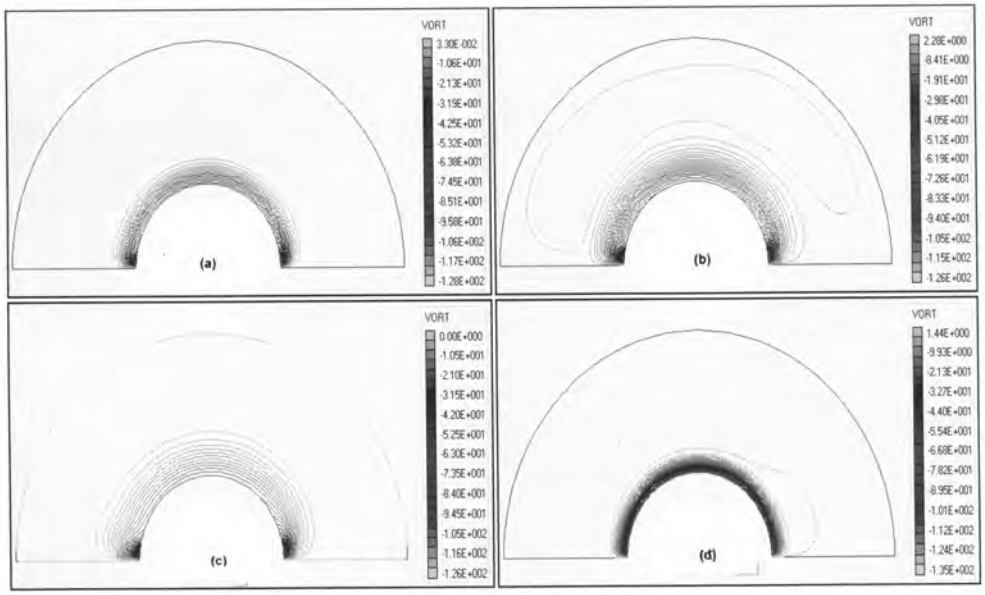

Figure 13. The lines of constant vorticity for R=10, α=4.5 at time levels (a) t=0.046 (b) t=0.1 (c) t=0.154 (d) t=0.993.

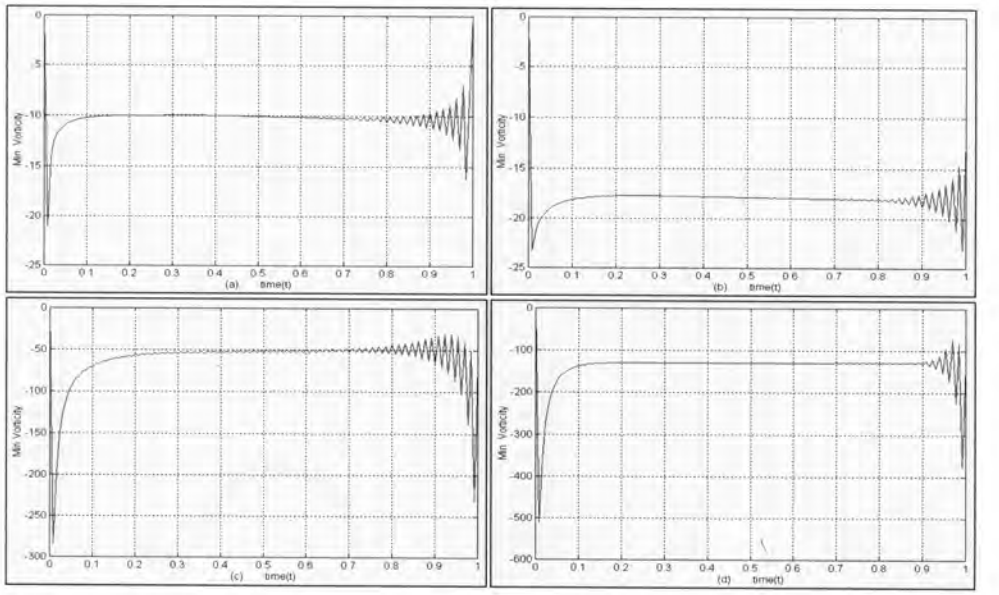

Figure 14. The variation of minimum value of vorticity E_{min} for (a)R=1, α=0 (b) R=1, α=4. 5 (c)R=349.285, α=2.5 (d) R=349.285, α=4. 5.

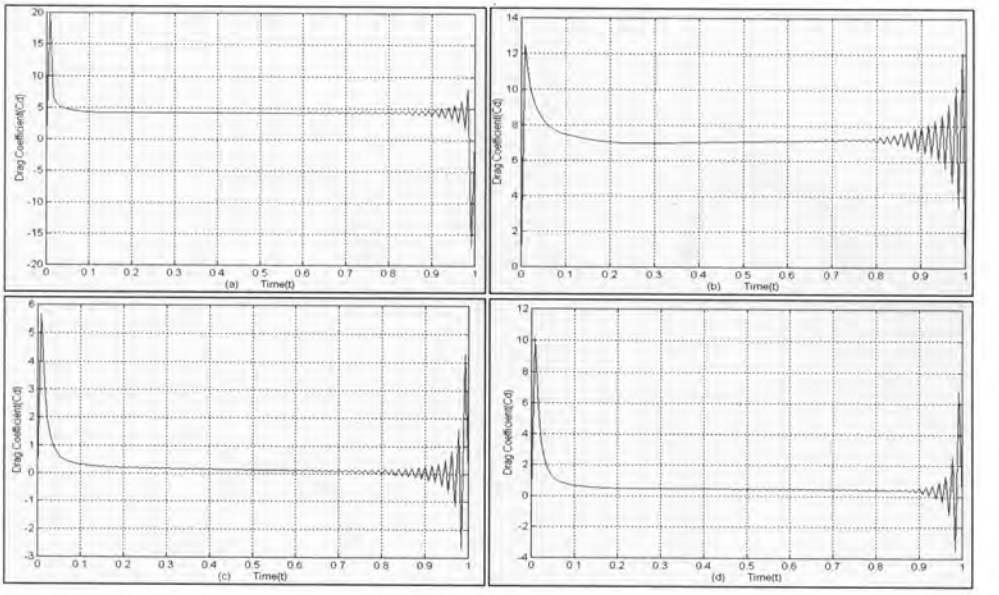

Figure 15. The variation of the drag over the surface of the cylinder for (a) α=0 (b) α=4. 5(c)R=349.285, α=2.5 (d) R=349.285, α=4. 5.

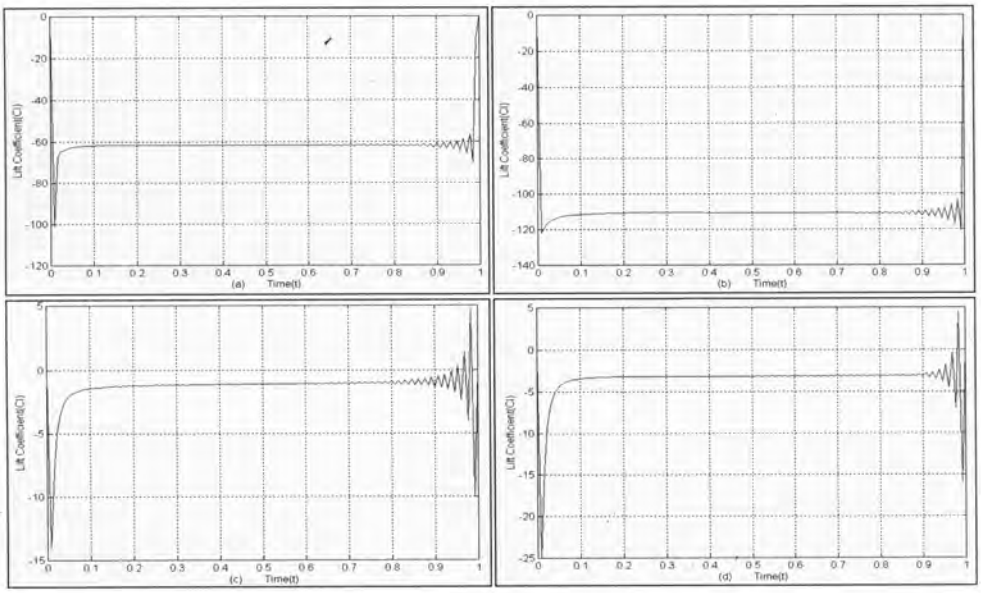

Figure 16. The variation of the lift over the surface of the cylinder for (a) α=0 (b) α=4. 5(c)R=349.285, α=2.5 (d) R=349.285, α=4.5.

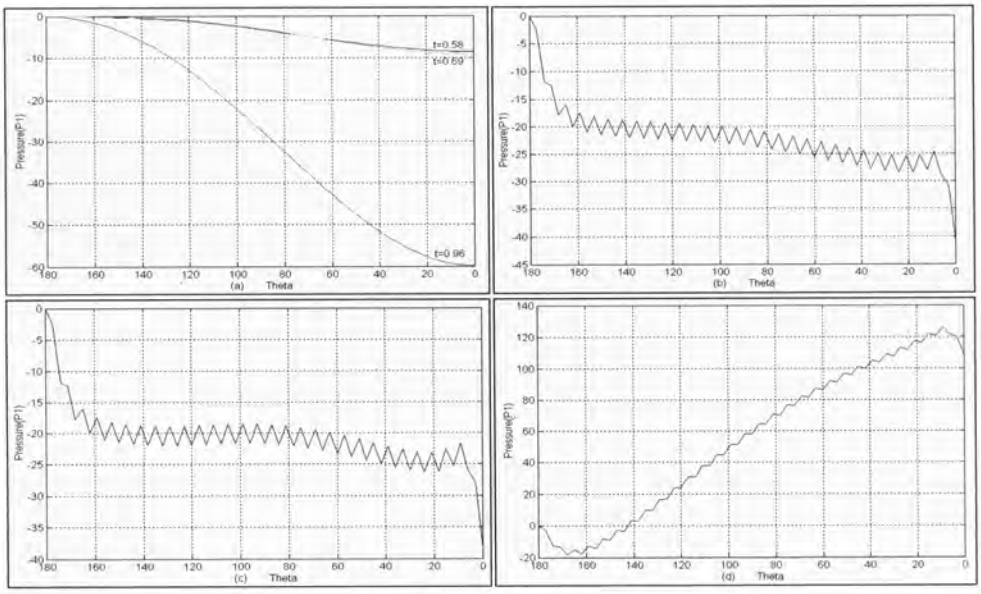

Figure 17. The variation of the pressure over the surface of the cylinder for R=349.285 (a) α=0 (b-d) α=4.5 at time levels t=0.58, 0.69, 0.96 respectively.

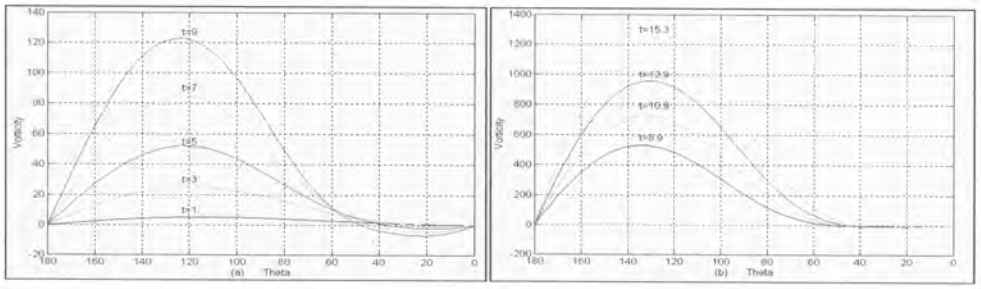

Figure 18. The variation of vorticity over the surface of a cylinder for smaller time for (a) R=10 (b) R=349.285 when α=0.

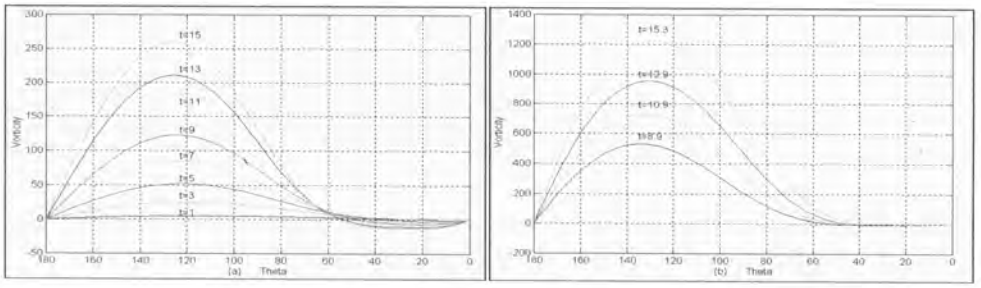

Figure 19. The variation of vorticity over the surface of a cylinder for larger time for (a) R=10 (b) R=349.285 when α=0.

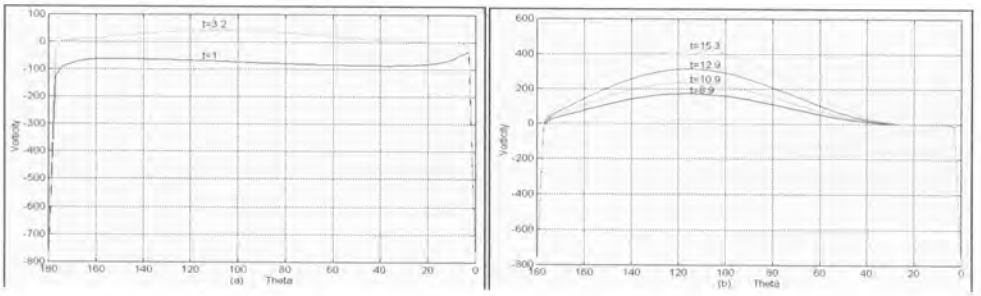

Figure 20. The variation of vorticity over the surface of a cylinder for R=349.285, α=4.5 (a) for smaller time (b) for larger time.

REFERENCES

1. Ackeret, J.(1925). Das Rotorschiff und Seine Physikalischen Grundlagen (Van denhoeck und Ruprecht, Göttingen.
2. Blasius, H.(1908). Z. Angew. Math. Phys., 56, 1.
3. Badr, H. M., Dennis, S.C.R.(1985). J. Fluid Mech., 185, 447.
4. Badr, H. M., Dennis, S.C.R.(1989). Computer and Fluids, 17(4), 579.
5. Cebeci, T.(1979). J. Comp. Phys, 31, 153.
6. Chang, C. and Chern, R. (1991). J. Fluid Mech., 233, 265.
7. Cichy, D. R., Harris, J.W.(1972). NASA, CR-2135.
8. Collins, W.M., Dennis, S.C.R. (1973). J. Fluid Mech., 60, 105.
9. Collins, W.M. and Dennis, S.C.R.(1974). J. Fluid Mech., 65(3), 461-480.
10. Dennis, S.C. R. (1960). Quart. J. Mech. Appl. Math. 13, 487.
11. Dommelen, L. L V., Shen, S.F. (1980). J. Comp. Phys. 38, 125.
12. Dommelen, L. L V. (1981). Ph.D. thesis, Cornell University.
13. Ece, M.C. (1984). Phy. Fluids, 27(5), 1077.
14. Goldstein, S. (1932). Proc.Lond. Math. Soc. (2), 34, 51.
15. Goldstein, S. and Rosenhead, L.(1936). Proc. Camb. Phil. Soc. 32, 392.
16. Görtler, H.(1944). Ing. Arch. 14, 286.
17. Görtler, H.(1948). Arch. Math. Karlsruhe, 1, 138.
18. Hildebrand, F. B.(1978).Introduction to Numerical Analysis, Tata McGraw Hill Publishing Co. Ltd.
19. Jain, M.K (1997). Numerical methods for scientific and engineering computation. New age international (pvt.) Ltd., Publishers.
20. Moore, F.K. (1958). Boundary layer Research, p296. Springer, Berlin.
21. Prandtl, L. (1925). Naturwissenschaften, 13, 93.
22. Prandtl, L., Tietjens, O.G. (1961). Applied Hydro and Aerodynamics. Dover, New York
23. Riley, N. (1975).SIAM Rev. 17, 274.
24. Sayers, A.T. (1979). Int. J. Mech. Elect. Engg., 7, 75.
25. Sears, W.R., Telionis, D.P. (1975). SIAM J. Appl. Math. 28, 215.
26. Tameda, S. (1972). Recent research on unsteady boundary layers, 2(ed. E.A. Eichel-brenner), 1165-1215. Quebec: Laval University Press.

27. Tennant, J.S.(1973). AIAA J. 11, 240.
28. Tennant, J.S., Johnson, W.S. and Krothapalli, A.(1976). J. Hydronaut 10, 102.
29. Walker, J.D.A.(1978). Proc. R. Soc. London Ser. A359, 1659.
30. Watson, E.J.(1957). Proc. Roy.Soc. A231, P104.

M. Anwar Kamal
Department of Mathematics, King Saud University, Riyadh, Saudi Arabia.
Abu Zar A. Siddiqui
UC ET, B. Z. University, Multan, Pakistan.

Date received May 27, 2003